MM Science Journal | www.mmscience.eu
ISSN 1803-1269 (Print) | ISSN 1805-0476 (On-line)
Special Issue | TEAM 2024
Transdisciplinary and Emerging Approaches to Multidisciplinary Science
11.9.2024 – 13.9.2024, Ostrava, Czech Republic
DOI: 10.17973/MMSJ.2024_10_2024068

TEAM2024-00008

EFFECT OF TUMBLING ON THE M300 MARAGING STEEL PARTS MADE BY SELECTIVE LASER MELTING

ABDESSELAM MECHALI[1], JOSEF HLINKA[2], JAKUB MESICEK[1], JIRI HAJNYS[1], JAN ZELINKA[1], DOMINIK KRISAK[1], LINKA CEPOVA[1], ROMAN BLAHA[1], ROBERT CEP[1], JANA PETRU[1]

[1] Department of Machining Assembly and Engineering Metrology, Faculty of Mechanical Engineering, VSB -Technical University of Ostrava, Czech Republic
[2] Department of Materials Engineering, Faculty of Materials and Technology, VSB-Technical University of Ostrava, Czech Republic
abdesselam.mechali.st@vsb.cz

Abstract
Increasingly, the fabrication of steel components is being done via 3D metal printing. One of the most commonly utilized reliable and precise methods is called selective laser melting (SLM), and it involves the use of metallic powder as the material that is fed into the laser. One of the famous problems that SLM technicians face is the roughness of the printed parts. The goal of this paper is to study the effect of tumbling on the M300 maraging steel, which was produced by using a Renishaw AM500 3D SLM printer. An examination of a procedure that is both cost-effective and efficient for manufacturing and surface treatment is carried out within the scope of this research. The post-processing was investigated in depth, which resulted in 2D surface roughness Ra = 0.39 µm and 3D surface roughness Sa = 0.4 µm. The topography and morphology of the specimens were checked. Additionally, the surface wettability was tested, and it was seen to display wetting behavior, the improvement in surface wettability caused a better surface energy.

Keywords:
3D printing, SLM, morphology, surface roughness, wettability, maraging steel, surface topography

1 INTRODUCTION

Designers can now produce practical, lighter, and considerably more sophisticated items from a variety of materials owing to 3D printing technology [Srivastava et al, 2023, Marsalek et al. 2020]. Metal components produced by selective laser melting (SLM) exhibited superior mechanical properties compared to those manufactured using traditional techniques [Bochnia et al. 2023, Liverani et al. 2017]. The aerospace, healthcare, and automotive industries use certain common alloys, and SLM technology has been specifically designed to work with these alloys. [Yakout et al. 2019, Chen et al. 2018, Mohammadian et al. 2018]. However, as mentioned in references [Strano et al. 2013, Wang et al. 2016, Leary et al. 2017, Liverani et al. 2022] one major drawback of 3D-printed objects, especially Selective Laser Melting (SLM) components, is the significant surface roughness resulting from the printing process. The location and orientation of the build chamber, the direction and rate of the inert gas stream, the characteristics of the powder, and the power and speed of the laser significantly affect the surface roughness of products created by selective laser melting (SLM) [Olakanmi 2013, Dedeakayogulları et al. 2022, Brytan et al. 2022, Mesicek et al. 2021, Mechali, et al. 2024]. The arithmetical mean height (Ra) for SLM components typically falls between 5 and 50 µm, with most instances being below 20 µm as referenced in [Vayssette et al. 2018, Townsend et al. 2016, Kaynak et al. 2018].
In order to get the needed surface roughness, small-scale manufacturing (SLM) components are required to go through the conventional computer numerical control (CNC) machining process. These two production techniques are merged into a hybrid additive-subtractive manufacturing (HASM) process, which involves simultaneously adding and subtracting material from a fabricated component using a single machine. [Mesicek et al. 2021, Du et al. 2016, Li et al. 2018]. Several post-processing techniques, including blasting, grinding, shot/ultrasonic peening, laser/electromechanical polishing, and others, have been investigated. Surface mechanical attrition treatment (SMAT) is a very efficient technique. The study conducted in [Sun et al. 2019] examined the surfaces of the selective laser melting (SLM) system portion, which were exposed to steel balls vibrating at a frequency of 40 Hz for a period of 10 minutes. This treatment resulted in a reduction of the surface roughness (Ra) from 15 to 1.8 µm. Increasing the duration of SMAT may lead to achieving a surface roughness of less than 0.5 µm. Using dry mechanical-electrochemical polishing (DMECP) in the [Bai et al. 2020] process resulted in decreasing the Ra to 0.75 µm.

In this study, to find a better post-processing method for reducing the roughness, we have tried tumbling. Specimens were created from M300 maraging steel powder by using the SLM Renishaw AM500 3D printer. The specimens were tumbled in three mediums, which are ceramic, plastic, and porcelain, for 180 minutes and 360 minutes, respectively. Following that, 2D and 3D roughness measurements were evaluated. After that, we evaluated the topography, morphology, and surface wettability of the printed samples.

2 MATERIAL AND METHOD

2.1 Powder characteristics

Carpenter Technology Corporation supplied the first M300 maraging steel powder. The manufacturer's provided chemical composition was verified using dispersive X-ray spectroscopy (EDS), as shown in Table 1. Minor discrepancies are noted, but due to the accuracy of both approaches, it is almost impossible to detect any variation from the expected composition.

Tab.1 : Chemical composition of the M300 maraging steel (Wt %).

Element	Ni	Co	Mo	Ti	Si	Fe
Manufacturer	17-19	7-10	4.50-5.20	0.30-1.20	0.08	Bal
EDS analysis	17.20	9.04	4.13	0.78	0.22	67.65

2.2 SLM and printing parameters

An SLM Renishaw AM500 3D printer, which is situated in Wotton-under-Edge, United Kingdom, was used in order to construct the samples. A laser that has a maximum power rating of 500 W is included in the machinery that makes up the printer. A purity level of 5.0 was achieved by the inert gas that was used, which was argon. 70 meters was the new focal size that was modified. For the purpose of preventing powder oxidation during the setup process and due to the ineffectiveness of the inert gas in removing metal vapors during the printing process, the chamber was continually purged of air and kept at a level that was lower than 1000 parts per million. QuantAM software, version 5.0.0.135, developed by Renishaw and Wotton under Edge in the United Kingdom, was used to set up the system. The samples were printed directly onto the substrate, the scanning strategy was meander as shown in Figure 1.b and there were need for support materials in building as shown in Figure 1.a. Three samples of dimension 43X10X3mm were printed in one build, as shown in Figure 1.c. The printing characteristics are resumed in table 2.

Tab.2 : Fabrication conditions for an SLM 3D printer.

Parameter	Value
The power of lasers	200 W
The strategy of printing	Meander
Hatch spacing	0.11 mm
The speed of scanning	650 mm/s
Preheating temperature	Ambient
Layer thickness	50 µm

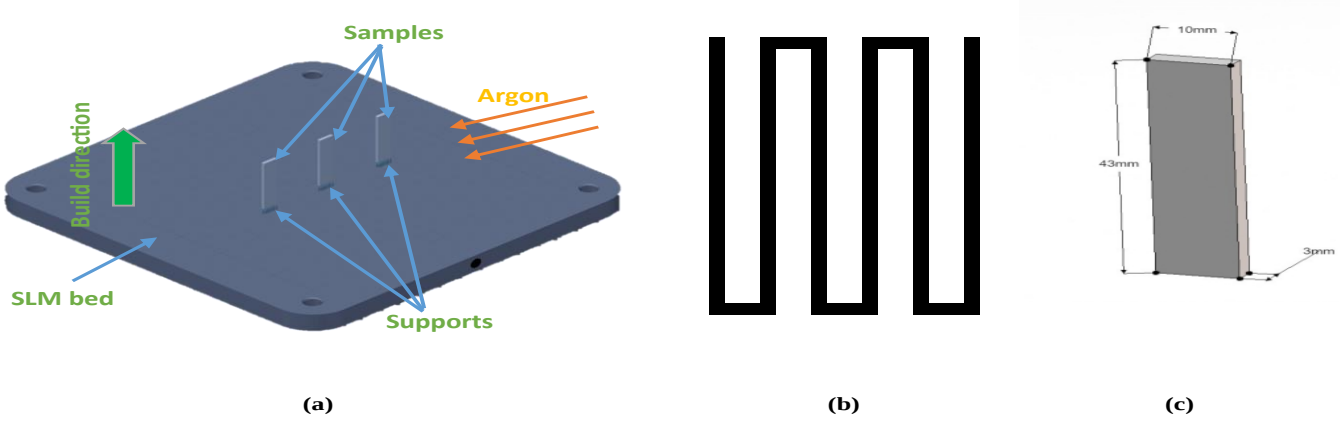

Fig. 1 : Schematic diagram showing the buildup of samples by SLM (a) SLM build (b) scanning strategy (c) sample characteristics.

2.3 Tumbling, measurements of surface roughness in 2D and 3D, and images of topography and morphology

After the manufacturing process, the specimens underwent tumbling using the OTEC CF1 32EL tumbler. The device was set to revolve at a velocity of 250 revolutions per minute. The tumbling process used three different materials: ceramic (DZS 10/10, Otec business, Pforzheim, Germany), plastic (XS 12K, Wather Trowal company, Germany), and porcelain (P 2/5, Otec company). Sample 1 was in its original state, whereas Sample 2 underwent a 60-minute tumbling procedure utilizing several types of tumbling material. The third and final sample underwent two full cycles in each tumbling medium, as shown in Table 3. Following that, the Alicona InfiniteFocus 5G optical microscope (IF MeasureSuite, Alicona Imaging GmbH, Raaba/Graz, Austria) was used to assess the 2D and 3D roughness of the surface as well as the topography images. Each sample surface of the three printed samples has been measured three times, and we have taken the mean value from each measurement with its standard derivation. Each sample had a scanned area of 7.3mm x 7.3mm. On the scanned sample, three areas measuring 2.5mm by 2.5mm were evaluated. For 2D roughness, the measured length was ln = 13 mm, and there were 3 measurements per sample. A cut-off filter was used according to the standard, i.e., for Ra 0.1 to 2 µm, a 0.8 mm filter was used. For Ra values of 2–10 µm, a 2.5 mm filter was used. Sample scan values were 20x lens was used. The lens can scan a surface with roughness: minimum measurable roughness (Ra) - 0.15µm and minimum measurable roughness (Sa) - 0.075µm, scanning distance: in horizontal was 0.438µmand in vertical 0.438µm, quality: lateral uncertainty x, y: 0.022µm.

Subsequently, a scanning electron microscope (SEM) was used to capture images of the surface microstructure's morphology.

Tab.3 : tumbling time of the M300 maraging steel samples.

Sample number	Tumbling mediums and time						Total time of tumbling
	Ceramic		Plastic		Porcelain		
	60 (min)	120 (min)	60 (min)	120 (min)	60 (min)	120 (min)	(min)
1							0
2	+		+		+		180
3		+		+		+	360

2.4 Surface wettability

The sample's wettability was assessed using the sessile drop technique. The surface contact angle was measured using the SEE system, and the free surface energy was determined using Advex Instrument software. Two microliter drops of double-distilled water were adhered to the surface under examination. The contact angle θ was measured by the tangent to the drop profile at the point where the three phases (liquid, solid, and gas) meet on the sample surface [Hlinka et al. 2020]. The free surface energy of the solid sample is calculated using Young's Equation (1), with γS, γSL, and γL denoting the interfacial tensions per unit length of the solid-vapor, solid-liquid, and liquid-vapor contact lines, respectively [Hlinka et al. 2020].

$$\gamma sv - \gamma sl = \gamma lv \cos \theta \qquad (1)$$

3 Results and discussion

3.1 2D, 3D surfaces roughness

The 2D surface roughness values are reported in Table 4, which shows these roughness levels as averages of as built and tumbling samples. It was found that the as-constructed sample has the mean value of the arithmetical means height Ra=5.60 µm, this value is inside the roughness field of the 3D printed samples (from 5 µm to 20 µm) as specified in [Mesicek et al. 2021] here we can conclude that M300 maraging steel has an ideal roughness for as built sample , and after 180 minutes of tumbling in three mediums, there was an improvement in the value of Ra, specifically by 89% (from 5.60 µm to 0.58 µm) and Rz, namely by 90% (from 38.24 µm to 5.93 µm), rather than Rt by 69% (from 51.37 µm to 16.18 µm). It was observed that increasing the time of tumbling in the sample by 360 minutes improved the 2D surface results by 93% (from 5.60 µm to 0.39 µm), Rz by 90% (from 38.24 µm to 3.92 µm), and Rt by 89% (from 51.37 µm to 5.54 µm). Further measurements of the 2D surface roughness showed an improvement in the value with increasing the time of tumbling. The overall surface roughness of specimens in their as built may be significantly reduced by the use of tumbling finishing. As it mentioned in [Mechali, et al. 2024] this occurs as a result of the tremendous amount of centrifugal force that is generated in high-energy systems as a result of the mixing of the compounds, which ultimately results in the smoothing out of the roughness in the printed specimens. Due to the fact that it is able to effectively avoid impacts and the damage that would otherwise be caused to the surfaces of the components, this option is considered to be safer.

The measurements of the 3D surface roughness values that are This parameter is an extension of the 2D surface roughness parameters, which were calculated as an average and adjusted to the nearest tenth, as shown in Table 5. In general, the tumbling method provided components with improved surface finishing. The roughness levels significantly decreased after the tumbling procedure. After 360 minutes of tumbling, Sa and Sq were confirmed to have decreased by at least 93% and 91%, respectively, to below 0.8 µm (0.4 µm, 0.73µm) after 360

minutes of tumbling simultaneously, Sz was lowered by 78% (24.97µm). Subsequent 3D tests showed an improved value after 360 minutes of tumbling this time consider as an appropriate time for tumbling for the M300 maraging steel which gives a high grade of the surface roughness. Analysis of the data revealed an inverse relationship between the duration of tumbling and the roughness values in both 2D and 3D, with every increasing of the time of tumbling the surface roughness decreased and become smoother. The 2D and 3D measurement values revealed a significant impact of tumbling on the SLM maraging steel printed samples. However, they were unable to provide a thorough understanding of the influence of tumbling on the surface. Consequently, we proceeded to analyze the topography photos of the samples in the next section.

Tab 4. 2D, surface roughness results after tumbling.

Parameter	Unit	As built sample	Sample with 180 minutes of tumbling	Sample with 360 minutes of tumbling
Ra	µm	5.60 ± 0.30	0.58 ± 0.025	0.39 ± 0.019
Rq	µm	7.40 ± 0.926	1.22 ± 0.24	0.77 ± 0.032
Rt	µm	51.37 ± 6.65	16.18 ± 3.68	5.54 ± 0.19
Rz	µm	38.24 ± 3.82	5.93 ± 1.43	3.92 ± 0.16
Rmax	µm	51.37 ± 9.33	16.18 ± 3.7	5.54 ± 0.19
Rp	µm	29.28 ± 2.14	2.48 ± 0.93	0.93 ± 0.44
Rv	µm	22.09 ± 4.57	13.69 ± 2.74	4.61 ± 0.24
Rc	µm	25.27 ± 3.46	11.25 ± 6.49	3.61 ± 0.053
Rsm	mm	376.06 ± 227.66	625.71 ± 361.25	689.13 ± 397.27
Rsk		0.51 ± 0.09	-5.84 ± 1.42	-2.94 ± 0.54
Rku		4.30 ± 0.82	56.10 ± 25.32	13.76 ± 2.16
Rdq		0.40 ± 0.04	0.05 ± 0.012	0.03 ± 0.00
Rt/Rz		1.34 ± 0.15	2.72 ± 0.28	1.41 ± 0.00
L	mm	7.21 ± 0.06	7.17 ± 0.009	7.16 ± 0.02
Lc	µm	2.5 ± 00	800 ± 00	800 ± 00

Tab 5. 3D, surface roughness results after tumbling.

Parameter	Unit	As built sample	Sample with 180 minutes of tumbling	Sample with 360 minutes of tumbling
Sa	µm	5.74 ± 0.13	1.29 ± 0.33	0.40 ± 0.03
Sq	µm	7.94 ± 0.20	1.93 ± 0.32	0.73 ± 0.05
Sp	µm	73.0 ± 5.17	5.37 ± 1.22	10.25 ± 3.72
Sv	µm	37.77 ± 5.81	41.71 ± 8.08	14.72 ± 1.07
Sz	µm	110.83 ± 1.78	47.08 ± 9.30	24.97 ± 3.68
S10z	µm	91.46 ± 3.14	36.89 ± 7.49	19.71 ± 2.59
Ssk		0.90 ± 0.04	-3.51 ± 0.86	-4.92 ± 0.33
Sku		7.2 ± 0.63	39.56 ± 1.03	45.55 ± 4.45
Sdq		0.68 ± 0.06	0.06 ± 0.00	0.04 ± 0.00
Sdr	%	16.85 ± 2.64	0.19 ± 0.01	0.08 ± 0.01
FLTt	µm	110.83 ± 1.78	47.08 ± 9.30	24.97 ± 3.86
Lc	mm	2.5 ± 00	0.8 ± 00	0.8 ± 00

3.2 3D surface topography images

In order to establish a clearer correlation between surface roughness and postprocessing, we captured three-dimensional photographs of each specimen, as seen in Figure 2. A suitable height scale was used for each measurement to enhance the visibility of the surface faults' maximum height and depth. The surface was leveled after scanning, and the images are raw without a filter. This is because the Lambda c (cut-off) filter is applied only when the roughness is measured afterwards. The 3D topography' photos depict the characteristics of the samples in their original state. The spatter phenomenon during printing has resulted in numerous peaks in Figure 2.a, which exhibits significant roughness. The maximum peak height within the selected area of sample Sp is measured at 73.06 µm, as shown in Table 5. During the 3D printing process, the evaporation led to the formation of multiple pores, referred

to as valleys. Consequently, the maximum depth of these valleys within the selected area is measured at Sv = 37.77 µm (table5). The combined effect of the peaks and valleys results in a maximum height of Sz = 110.83 µm (table5). Upon tumbling in each medium for a duration of 60 minutes, specimen 2 exhibited a significant reduction in roughness, as seen in Figure 2.b. This reduction resulted in a minimal number of peaks, finally leading to an improved peak-to -valley ratio of Sz = 33.49 µm (table5). One might infer that the integration of the three media resulted in the formation of a seamless surface. Furthermore, it was seen that the process of tumbling resulted in the formation of a new bottom layer, as shown in Figure 2.c. The depth of the holes was decreased as a result of this new layer, which resulted in improved surface roughness and a surface that was much buried. The suggested treatment technique resulted in a significant reduction in the peaks and valleys of the as-built surfaces that were being transformed. In the process of recording, the roughness reduction of Sz was found to be 24.97 µm (table5).

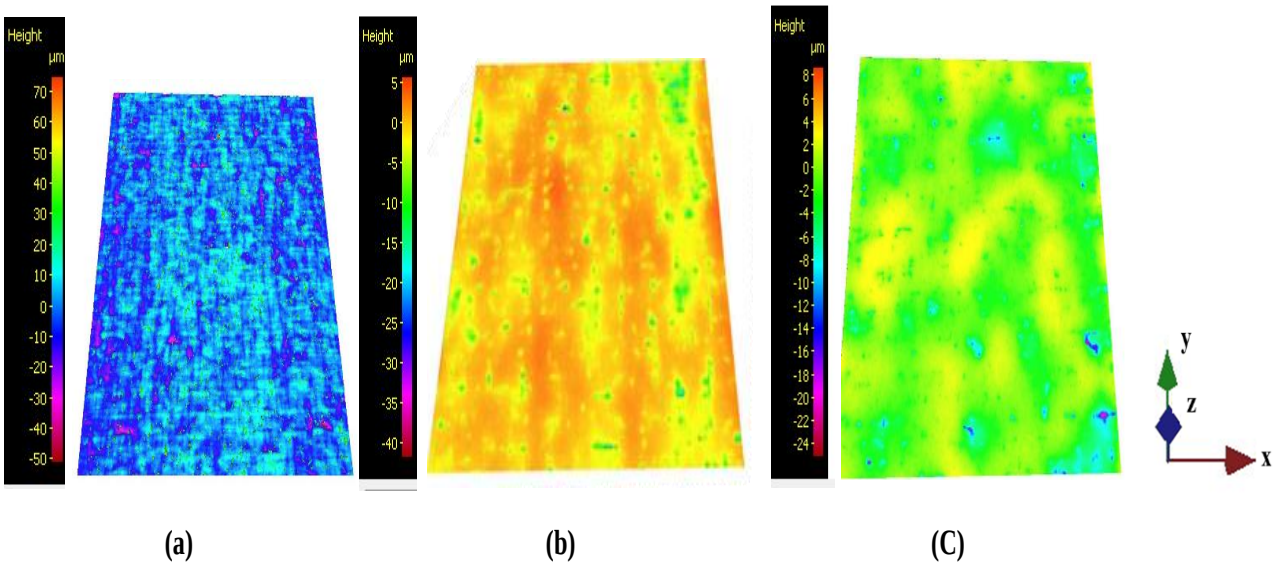

Fig.2: surface topography improvement with tumbling (a) as built (b) specimen with 180 minute of tumbling (c) specimen with 360 minutes of tumbling.

3.3 Morphology of the tumbled samples

The mechanical properties of metal components vary significantly based on their microstructure, which includes aspects such as phase type, grain size and shape, dendritic structure, and element segregation. Scanning electron micrographs provide evidence of a tumbling method for each sample and highlight the differences in the scanned surfaces depending on the technology used to tumble the components. Figure 3 provides optical microscope images depicting the microstructure of SLM components after completion of finish machining at different feed rates. The photographs illustrate the samples subjected to centrifugal tumbling and vibratory tumbling. The scale of the pictures was 500 µm, 100 µm, and 20 µm, respectively. The items shown are presented in Figure 3.1. With respect to the as-built specimens, we noted the presence of dislodged particles (Fig 3.1.a), particles that were only partly melted (Fig. 3.1.b), fractures (Fig. 3.1.c), melt satellites (Fig. 3.1.c). and pores (Figure 3.1.c). These faults arose from the physical phenomena inherent in the printing process.

After being tumbled for a length of 180 minutes, the surface of the specimen, as seen in figure 3.2, shows a noticeable decrease or smoothing of the roughness peaks. As a result, the surface seems far more even, but some of the original depressions still remain. Nevertheless, after undergoing a 180-minute tumbling process in different mediums, certain remains satellites and melt powder persisted on the surface, as seen in figure 3.2.c. we can conclude here that tumbling M 300 maraging steel in the three mediums for 60 minutes each is not enough to have a proper surface.

Figure 3.3 illustrates that a significant proportion of remain satellites were eliminated when subjected to a 360-minute tumbling sample. Furthermore, a substantial segment of the valley had a reduction in Sv, specifically to a value of 14.725 µm, as shown in Table 5, which consequently led to a more polished and lustrous surface. This concerns the impact of tumbling duration on the surface. The topmost layer of the surface was removed, and a new layer of surface was created, this new layer created as reason of deleting the top layer, the interaction between the medium and the samples, leading to a reduction in the indentations as shown in table 5 the peak to the valley Sz reduced from 110.83 µm to 24.97 µm. Nevertheless, a full tumbling of 360 minutes is often accepted as an appropriate time for eliminating the spherical particle.

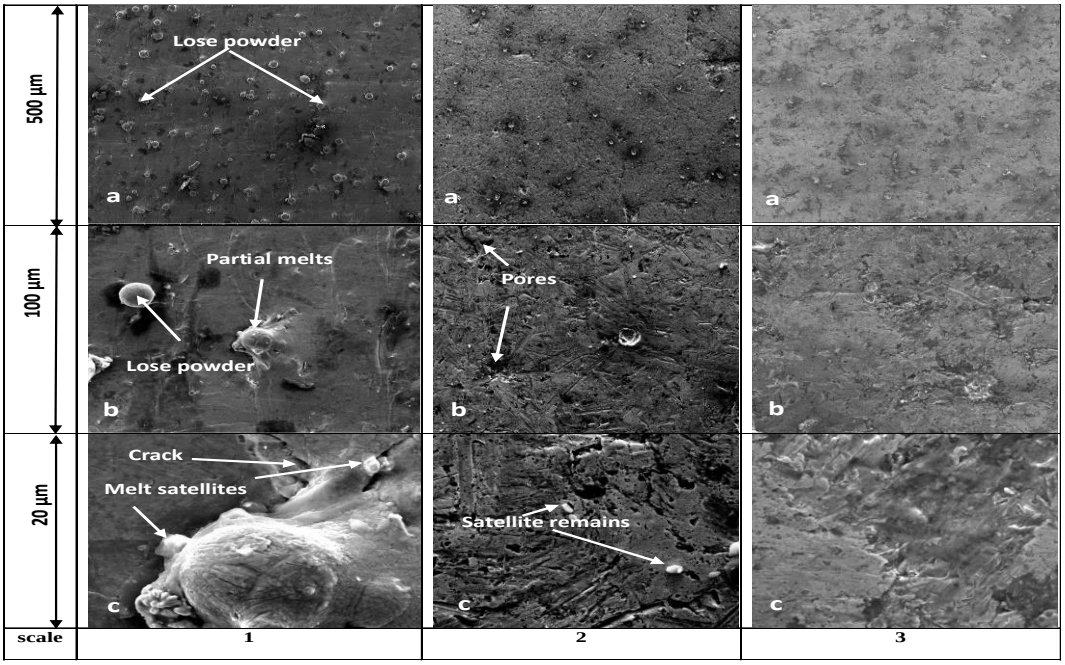

Fig. 3: surface microstructure morphology tumbling (1) as built (2) specimen with 180 minute of tumbling (3) specimen with 360 minutes of tumbling.

3.4 Surface wettability

Table 6 offers a presentation of the average findings of this test together with their respective standard deviations. Images that are representative of droplets on surfaces that have been examined are seen in Figure 4.a (the sample as it was produced) and Figure 4.b (the sample that was tumbled 360 minutes). In comparison to the as-built sample, which has the same surface character, the tumbled sample exhibits a surface wettability property that is much greater. A different value of surface energy was also produced as a consequence of this, where the surface energy increased with a decrease in the contact angle. Both the as built and post-processed samples have wetting behavior where the contact angle is under 90.

Tab.6: Values of contact angle and calculated surface energy for as built sample and tumbled sample.

Specimen	Contact Angle (◦)	Surface Energy (mJ.m−2)	Wetting Behavior
As built sample	72.27 ± 6.88	40.33	Wetting
Tumbled sample	57.85 ± 4.27	45.29	Wetting

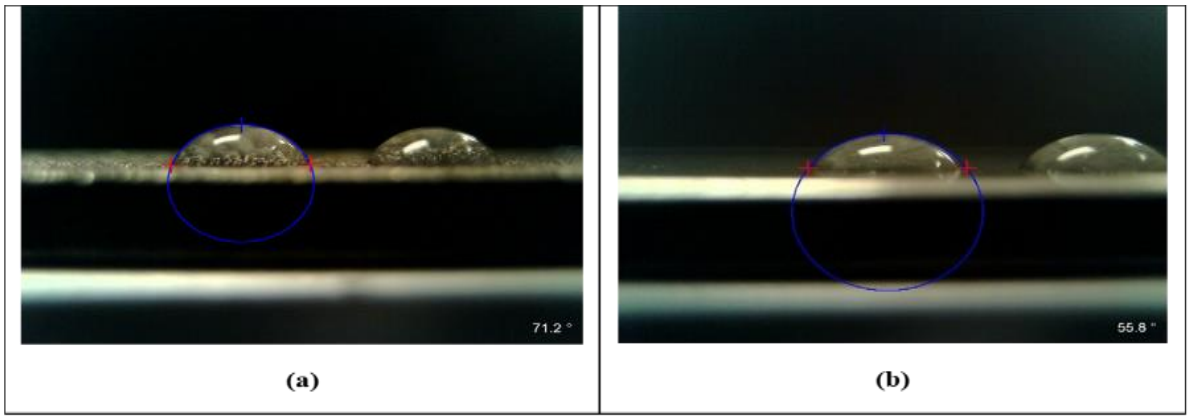

Fig. 4: contact angles with centrifugal tumbling (a) as built specimen (b) post treated specimen

4 CONCLUSION

The goal of this study was to investigate the effect of tumbling on the virgin M300 maraging steel 3D printed parts using SLM. In terms of roughness as well as topography, morphology, and surface wettability, the results of this study can be summarized as follows:

- 2D and 3D roughness measurements showed that tumbling improved the 2D roughness parameters until Ra = 0.39 µm, Rz = 3.92 µm, and 3D parameters Sa = 0.40 µm and Sz = 24.97 µm. In addition, it was found that the as-constructed sample has the mean value of the arithmetical means height Ra = 5.60 µm, this value in the internal of the average SLM printed roughness (from 5 µm to 20 µm) as it was mentioned in previous studies.

- 3D topography pictures demonstrated that tumbling effectively eliminated peaks up to Sp = 10.25 µm, eliminating peaks reduced valleys to Sp = 14.72 µm, resulting in a total peak in valley Sz = 24.97 µm.,

- Scanning electron microscopy (SEM) images demonstrate the effect of tumbling on the surface, effectively eliminating partial melts powder, melt satellites, melt powder remains, cracks, while also reducing the size of the pores and valleys.

- Measurements of the contact angles showed that the SLM-printed sample has a wetting behavior (contact angle under 90); however, post-processing improved the surface wettability of the M300-printed material, which led to an improvement in surface energy.

With these results, we conclude that tumbling is highly recommended for post-processing applications of M300 maraging steel in aerospace, medical instruments, the automotive industry, and general industry in order to reduce the roughness.

.

3 ACKNOWLEDGMENTS

This paper was completed in association with the project Innovative and additive manufacturing technology - new technological solutions for 3D printing of metals and composite materials, reg. no. CZ.02.1.01/0.0/0.0/17_049/0008407 financed by Structural Funds of the European Union. The article has been done in connection with the project Students Grant Competition SP2023/088 „Specific Research of Modern Manufacturing Technologies for Sustainable Economy “financed by the Ministry of Education, Youth and Sports and Faculty of Mechanical Engineering VŠB-TUO.

4 REFERENCES

[Bochnia el al. 2023] Bochnia, J.; Kozior, T.; Zyz, J. The Mechanical Properties of Direct Metal Laser Sintered Thin-Walled Maraging Steel (MS1) Elements. Materisals.16, 4699 (2023).

[Brytan et al. 2022] Brytan, Z.; Król M.; Benedyk , M.; Pakieła,W.; Tanski, T.; Jemberu Dagnaw M.; Snopinski, P.; Pagác, M.; Czech A. Microstructural and Mechanical Properties of Novel Co-Free Maraging Steel M789 Prepared by Additive Manufacturing. Materials. 15(5), 1734(2022),

[Bai et al. 2020] Bai, Y.; Zhao, C.; Yang, J.; Fuh, J.; Lu, W.; Weng, C.; Wang, H. Dry mechanical-electrochemical polishing of selective laser melted 316L stainless steel. Materials. 193, 108840(2020).

[Chen et al. 2018] Chen, Z.; Wu, X.; Tomus, D.; Davies, C. surface roughness of selective laser melted ti-6al-4v alloy components. Additive Manufacturing. 21, 91–103(2018).

[Dedeakayogulları et al. 2022] Dedeakayogulları, H.; Kaçal, A.; Keser, K. Modeling and prediction of surface roughness at the drilling of SLM-Ti6Al4V parts manufactured with pre-hole with optimized ANN and ANFIS. Measurement. 203, 112029 (2022).

[Du et al. 2016] Du, W.; Bai, Q.; Zhang, B. A Novel Method for Additive/Subtractive Hybrid Manufacturing of Metallic Parts. Procedia Manufacturing. 5, 1018–1030(2016).

[Hlinka et al. 2020] Hlinka, J.; Kraus, M.; Hajnys, J.; Pagac, M.; Petru, J.; Brytan, Z.; Tanski, T. Complex Corrosion Properties of AISI 316L Steel Prepared by 3D Printing Technology for Possible Implant Applications. Materials, 13(7), 15-27(2020).

[Kaynak et al. 2018] Kaynak, Y.; Kitay, O. Porosity, Surface Quality, Microhardness and Microstructure of Selective Laser Melted 316L Stainless Steel Resulting from Finish Machining. Journal of Manufacturing and Material Processing. 2, 36(2018).

[Leary et al. 2017] Leary, M. Surface Roughness Optimisation for Selective Laser Melting (SLM): Accommodating Relevant and Irrelevant Surfaces; RMIT University, Centre for Addictive Manufacturing: Melbourne, VIC, Australia; pp. 99–118(2017).

[Liverani et al. 2022] Liverani, E.; Li, Y.; Ascari, A.; Zhao, X.; Fortunato, A. The effect of femto-second laser shock peening on the microstructures and surface roughness of AlSi10Mg samples produced with selective laser melting (SLM). 6th CIRP Conference on Surface Integrity. 108, 77–81 (2022).

[Liverani et al. 2017] Liverani, E.; Toschi, S.; Ceschini, l.; Fortunato, A. Effect of selective laser melting (SLM) process parameters on microstructure and mechanical properties of 316L austenitic stainless steel. Journal of Materials Processing Technology. 249, 255–263(2017).

[Li et al. 2018] Li, L.; Haghighi, A.; Yang, Y. A novel 6-axis hybrid additive-subtractive manufacturing process: Design and case studies. Journal of Manufacturing and Material Processing. 33, 150–160(2018).

[Marsalek et al. 2020] Marsalek, P.; Sotola, M.; Rybansky, D.; Repa, V.; Halama, R.; Fusek, M.; Prokop, J. Modeling and Testing of Flexible Structures with Selected Planar Patterns Used in Biomedical Applications. Materials. 14(1), 140(2020).

[Mohammadian et al. 2018] Mohammadian, N.; Turenne, S.; Brailovski, V. Surface finish control of additively-manfactured Inconel 625 components using combined chemical-abrasive flow polishing. Journal of Materials Processing Technology. 252, 728–738(2018).

[Mesicek et al. 2021] Mesicek, J., Ma, Q.-P., Hajnys, J., Zelinka, J., Pagac, M., Petru, J., & Mizera, O. (2021). Abrasive Surface Finishing on SLM 316L Parts Fabricated with Recycled Powder. *Applied Sciences*, *11*(6), 2869. https://doi.org/10.3390/app11062869

[Mechali, et al. 2024] Mechali, A; Mesicek, J; Ma, Q.-P; Hajnys, J; Gautam, P; Blaha, R; Krisak, D, Petru, J. 2024.Abrasive Surface Treatment of Alsi10mg Aarts made by L-PBF. MM Science Journal. 7165-7172(2024).

[Olakanmi 2013] Olakanmi, E. Selective laser sintering/melting (SLS/SLM) of pure Al, Al–Mg, and Al–Si powders: Effect of processing conditions and powder properties. Journal of Materials Processing Technology. 213, 1387–1405(2013).

[Srivastava et al. 2023] Srivastava, A.; K., Kumar, A.; Kumar, P.; Gautam, P.; Dogra, N. Research Progress in metal additive manufacturing: Challenges and Opportunities. International Journal on Interactive Design and Manufacturing. 1-17(2023).

[Strano et al. 2013] Strano, G.; Hao, L.; Everson, R.; Evans, K. Surface roughness analysis, modelling and prediction in selective laser melting, Journal of Materials Processing Technology. 213, 589–597(2013).

[Sun et al. 2019] Sun, Y.; Bailey, R.; Moroz, A. Surface finish and properties enhancement of selective laser melted 316L stainless steel by surface mechanical attrition treatment. Surface and Coating Technology. 378, 124993(2019).

[Townsend et al. 2016] Townsend, A.; Senin, N.; Blunt, L.; Leach, R.; Taylor, J. Surface texture metrology for metal additive manufacturing: A review. Procedia Engineering. 46, 34–47(2016).

[Vayssette et al. 2018] Vayssette, B.; Saintier, N.; Brugger, C.; Elmay, M.; Pessard, E. Surface roughness of Ti-6Al-4V parts obtained by SLM and EBM: Effect on the High Cycle Fatigue life. Procedia Engineering. 213, 89–97(2018).

[Wang et al. 2016] Wang, D.; Liu, Y.; Yang, Y.; Xiao, D. 2016, Theoretical and experimental study on surface roughness of 316L stainless steel metal parts obtained through selective laser melting. Rapid Prototyping Journal. 22, 706–716(2016).

[Yakout et al. 2019] Yakout, M.; Elbestawi, M.; Veldhuis, S. Density and mechanical properties in selective laser melting of Invar 36 and stainless steel 316L. Journal of Materials Processing Technology. 266, 397–420(2019).

Mechali Abdesselam
VSB-Technical University of Ostrava
Faculty of Mechanical Engineering Department of Machining Assembly and Engineering Metrology
17. listopadu 2172/15, Ostrava, 708 00, Czech Republic
abdesselam.mechali.st@vsb.cz